A Fluorescent α-Factor Analogue Exhibits Multiple Steps on Binding to Its G Protein Coupled Receptor in Yeast†

Anshika Bajaj,‡ Andjelka Ćelić,‡ Fa-Xiang Ding,§ Fred Naider,§ Jeffrey M. Becker,|| and Mark E. Dumont*,‡

Department of Biochemistry and Biophysics, University of Rochester School of Medicine and Dentistry, P.O. Box 712, Rochester, New York 14642, Department of Chemistry, College of Staten Island and Macromolecular Assemblies Institute of the City University of New York, New York, New York 10314, and Department of Microbiology, University of Tennessee, Knoxville, Tennessee 37996

Received March 28, 2004; Revised Manuscript Received August 4, 2004

ABSTRACT: The yeast α-factor receptor encoded by the *STE2* gene is a member of the extended family of G protein coupled receptors (GPCRs) involved in a wide variety of signal transduction pathways. We report here the use of a fluorescent α-factor analogue [K^7(NBD), Nle^{12}] α-factor (Lys^7 (7-nitrobenz-2-oxa-1,3-diazol-4-yl), norleucine^{12} α-factor) in conjunction with flow cytometry and fluorescence microscopy to study binding of ligand to the receptor. Internalization of the fluorescent ligand following receptor binding can be monitored by fluorescence microscopy. The use of flow cytometry to detect binding of the fluorescent ligand to intact yeast cells provides a sensitive and reproducible assay that can be conducted at low cell densities and is relatively insensitive to fluorescence of unbound and nonspecifically bound ligand. Using this assay, we determined that some receptor alleles expressed in cells lacking the G protein α subunit exhibit a higher equilibrium binding affinity for ligand than the same alleles expressed in isogenic cells containing the normal complement of G protein subunits. On the basis of time-dependent changes in the intensity and shape of the emission spectrum of [K^7(NBD),Nle^{12}] α-factor during binding, we infer that the ligand associates with receptors via a two-step process involving an initial interaction that places the fluorophore in a hydrophobic environment, followed by a conversion to a state in which the fluorophore moves to a more polar environment.

Cellular receptors respond differently to different ligands. Agonists promote activation of signaling pathways, whereas antagonists and inverse agonists may be closely related chemical compounds that bind to the same receptors but either inhibit signaling or fail to induce a response. In general, the mechanisms by which ligand binding leads to either activation or inhibition of receptor signaling remain poorly understood. However, various models have been proposed to account for the fact that activation of the signal transduction must result from some steps beyond simple binding of ligand to receptors (*1*−*6*).

Yeast pheromone receptors are members of the broadly distributed class of G protein coupled receptors (GPCRs)[1] that promote exchange of GTP for GDP on intracellular trimeric G proteins in response to a variety of ligands, including neurotransmitters, hormones, ions, and sensory stimuli. The yeast receptors are used for detecting the peptide pheromones secreted by the two types of haploid yeast cells, initiating physiological responses and cell cycle arrest in preparation for mating to form a diploid zygote. The α-factor receptor encoded by the yeast *STE2* gene is found on *MAT***a** cells. It binds to α-factor, a 13-residue peptide pheromone with the sequence WHWLQLKPGQPMY that is secreted by cells of the *MAT*α mating type. The **a**-factor receptor, encoded by the *STE3* gene, allows cells of the *MAT*α type to respond to **a**-factor, a 12 residue farnesylated (*7*, *8*) peptide secreted by cells of the *MAT***a** type.

Numerous peptide analogues of α-factor have been synthesized and tested for their effects on the yeast pheromone response (*9*−*12*). Binding of α-factor and related analogues has generally been assessed using radiolabeled α-factor produced by biosynthetic incorporation of ^{35}S methionine, by reductive tritiation of an α-factor analogue, or by iodination of a tyrosine-containing α-factor analogue (*13*−*16*). The use of a fluorescent ligand-binding assay can provide advantages for the analysis of receptor structure and function that include the ability to conduct real-time assays of binding kinetics and the possibility of conducting high-throughput screens for alterations in receptors and ligands that affect binding. While the synthesis of fluorescent α-factor derivatives has been reported (*17*−*19*), the level of fluorescence has generally been too low and the nonspecific background too high to allow accurate quantitation of binding to receptors on cells or membranes.

The fluorescent α-factor analogue [K^7(NBD),Nle^{12}] α-factor binds to the α-factor receptor with high affinity and activates the pheromone response with a potency only

† Supported by NIH Grants GM59357 (to M.E.D.) and GM22086 and GM22087 (to F.N. and J.M.B.). Fred Naider is currently the Leonard and Esther Kurtz Term Professor at the College of Staten Island.

* Corresponding author. Phone: 585-275-2466. Fax: 585-271-2683. E-mail: Mark_Dumont@urmc.rochester.edu.

‡ University of Rochester School of Medicine and Dentistry.

§ College of Staten Island and Macromolecular Assemblies Institute of the City University of New York.

|| University of Tennessee.

[1] Abbreviations: GPCR, G protein coupled receptor; [K^7(NBD), Nle^{12}] α-factor, Lys^7(7-nitrobenz-2-oxa-1,3-diazol-4-yl), norleucine^{12} α-factor; HA, hemagglutinin.

10.1021/bi0494018 CCC: $27.50
Published on Web 09/29/2004

slightly less than that of native α-factor. It contains a relatively small fluorophore, NBD, that does not significantly interfere with receptor binding and is very sensitive to the polarity of its environment, resulting in a large increase in fluorescence on moving from aqueous solution to nonpolar solvents or the receptor binding site (*18*, *19*). In previous attempts to use this compound as the basis for a fluorescent binding assay, a high concentration of cells or membranes was needed to provide a detectable signal from bulk suspensions in a conventional fluorimeter (*18*). This meant that a high total concentration of ligand was needed to saturate the binding sites, making it difficult to conduct binding assays at a low concentration corresponding to the dissociation constant for the interaction, as is needed to define the binding parameters. Extensive studies of the interactions of fluorescent ligands with receptors by Sklar and colleagues have demonstrated that analysis of cell-associated fluorescence by flow cytometry can circumvent many of the problems brought about by low fluorescence signals and high backgrounds from unbound ligand (*20*−*22*). The usefulness of flow cytometry for characterizing binding of ligands to antibodies expressed on yeast cells has been demonstrated by Wittrup and co-workers (*23*).

We report here the use of fluorescence microscopy and flow cytometry to enhance detection of receptor-bound ligand containing the environmentally sensitive fluorophore NBD conjugated to Lys7 of α-factor. The increased sensitivity of the flow cytometry-based assays allows determination of equilibrium and kinetic constants characterizing ligand binding and internalization of ligand. The kinetic analysis suggests that α-factor associates with the receptor via a two-stage process consisting of an initial binding event followed by a rearrangement of the ligand−receptor complex.

EXPERIMENTAL PROCEDURES

Plasmids. Multicopy plasmid pMD1003 expressing full-length *STE2* with an HA epitope tag was constructed by introducing an *Xho*I site after the influenza hemagglutinin (HA) epitope in pMD240 (*24*) by site-directed mutagenesis with ON504 (5′-CTT TTT CAA AGC CGT AAA TCT CGA GCC GCG GCC GCC CTG AGC AGC GTA ATC-3′). To make the multicopy plasmid pMD1098 expressing a full-length receptor with a c-myc epitope, a *Sac*1−*Sph*1 insert containing the c-myc tagged *STE2* allele from pMD357 (*25*) was ligated into *Sac*1−*Sph*1-cut pMD228, a vector containing 2μ replication sequences and a URA3 marker (*24*). The same *Sac*1−*Sph*1-cut insert was ligated into the *Sac*1−*Sph*1-cut pFL38 (*26*) to obtain the *URA3 CEN* plasmid pMD1145 encoding full-length receptor with a c-myc epitope. Both pMD1098 and pMD1145 contained a replacement of alanine for an asparagine at position 430, immediately adjacent to the site of fusion to the epitope. This replacement does not affect the properties of the receptor (*25*, *27*).

C-terminal-truncated Ste2p containing a C-terminal c-myc epitope tag was expressed from the multicopy plasmids pMD1055 and pMD1230. To create pMD1055 a *Nhe*1−*Sac*1 fragment (1574 bases) from pMD626 was inserted into *Nhe*1−*Sac*1-cut pMD240, yielding pMD985. Plasmid pMD626 was made by site-directed mutagenesis of plasmid pMD423 (*28*) with oligonucleotide ON308 (5′-GCT TTT GCT CAG AGC GGC CGC CTT TGG ATG CAT TAT TAG C-3′) deleting residues from Thr305 to the *STE2* C-terminus. An *Xho*I site was introduced after the c-myc epitope in pMD985 by site-directed mutagenesis with ON512 (5′-CAA AGC CGT AAA TTT TGA TCT CGA GCC GCT ACT ATT AAG ATC CTC CTC GGA-3′) yielding pMD1055. The truncated receptor encoded by this plasmid had cysteine at position 252 replaced with a serine. To make a multicopy plasmid bearing native truncated receptor, a *Nhe*1−*Kpn*1 fragment from pMD1003 was ligated into *Nhe*1−*Kpn*1-cut pMD1055 to obtain pMD1230. To make the *CEN* plasmid pMD1231, containing the native truncated receptor, a *Sac*1−*Sph*1 fragment from pMD1230 was ligated into *Sac*1−*Sph*1-cut pMD149 (*24*). Replacement of cysteine at position 252 by a serine has no significant effect on receptor function or binding (results not shown and refs *28*−*30*).

The plasmid pMD235 allowing deletion of the *STE4* gene was made as follows: A *Sac*1−*Sph*1 fragment carrying *STE4* was cut from pMD212 (*24*) and inserted into *Sac*1−*Sph*1-cut pUC19 to obtain pMD213. pMD213 was then cut with *Bsr*G1, removing almost all the *STE4* coding region, and resealed using ON73 (5′-GTA CAG GAT CCT-3′) to introduce a *Bam*HI site at the site of the deletion. The resulting plasmid, pMD217, was then cleaved with *Bam*H1 and a *Bgl*1−*Bam*H1 fragment containing the HisG−*URA3*−HisG disruption cassette (*31*) was inserted, yielding pMD235.

Yeast Strains and Media. The yeast strains used in this paper are summarized in Table 1. The original *ste2*-Δ host strain used was A232 (*MATa ste2*-Δ *bar1*$^-$ *cry1*^{R} *ade2-1 his4-580 lys2*$_{oc}$ *tyr1*$_{oc}$ *SUP4-3*^{ts} *leu2 ura3 FUS1::p[FUS1-lacZ TRP1*]). Yeast transformations were performed by the method of Chen et al. (*32*). Yeast were cultured on dropout media or YPD as described (*33*). To test the effect of varying receptor and G protein expression on binding parameters, multi- or single-copy *URA3*-containing plasmids expressing full-length or truncated receptors were cotransformed into the *ste2*-Δ *far1*$^-$ strain A575 (*25*) with pMD284 (yEPlac181, *34*), a multicopy *LEU2* vector containing no insert. These plasmids were also transformed into a *ste2*-Δ *gpa1*-Δ *far1*$^-$ strain A1017, which was constructed by transforming strain A575 with *Kpn*1−*Xba*1-cut pMD398 and popping out on FOA (5-fluoroorotic acid) as described previously (*24*). The multicopy plasmids expressing the full-length and the truncated receptors were also transformed into a *ste2*-Δ *ste4*-Δ *far1*$^-$ strain, A2951 that was constructed by transforming the *ste4*-Δ *far1*$^-$ strain A570 with *Pml*1-digested pMD147 (*24*) and popping out on FOA to delete *STE2*. A570 was derived from the *STE4*$^+$ strain A294 (*24*) by transforming with a *Sac*1−*Sph*1-cut pMD235 and popping out on FOA.

Preparation and Assay of Fluorescent Ligand Solutions. [K^7(NBD),Nle^{12}] α-factor and [Orn^7(NBD),Nle^{12}] α-factor were prepared as described previously (*18*). To prepare stock solutions of ligand, a small amount of the relevant ligand was first dissolved in 150 μL of methanol; then 150 μL of water was added. The absorbance of the ligand solution was measured at 470 nm, and the concentration of the stock solution was calculated by using an extinction coefficient at 470 nm of 23 000 M^{-1} cm^{-1}. Owing to the light-sensitive nature of the fluorescent peptide, the solution was protected from light during and after preparation and stored in the dark. Subsequent ligand dilutions were made in a solution of

Table 1: Yeast Strains Expressing Full-Length and Truncated Receptors

yeast strain	*STE2* allele	*GPA1* allele	*STE4* allele	plasmids	yeast host strain	receptor epitope
A2933	*CEN* Ste2p[a]	*GPA1*$^+$	*STE4*$^+$	pMD1145	A232	c-myc
A2737	*CEN* Ste2p[a]	*GPA1*$^+$	*STE4*$^+$	pMD1145 + pMD284	A575	c-myc
A2738	*CEN* Ste2p[a]	*gpa1*-Δ	*STE4*$^+$	pMD1145 + pMD284	A1017	c-myc
A2927	*CEN* Ste2p(Δ305−431)	*GPA1*$^+$	*STE4*$^+$	pMD1231	A232	c-myc
A2728	multicopy Ste2p[a]	*GPA1*$^+$	*STE4*$^+$	pMD1098	A232	c-myc
A2735	multicopy Ste2p[a]	*GPA1*$^+$	*STE4*$^+$	pMD1098 + pMD284	A575	c-myc
A2733	multicopy Step[a]	*gpa1*-Δ	*STE4*$^+$	pMD1098 + pMD284	A1017	c-myc
A2962	multicopy Ste2p[a]	*GPA1*$^+$	*ste4*-Δ	pMD1098 + pMD284	A2951	c-myc
A2662	multicopy Ste2p(Δ305−431)[b]	*GPA1*$^+$	*STE4*$^+$	pMD1055	A232	c-myc
A2912	multicopy Ste2p(Δ305−431)	*GPA1*$^+$	*STE4*$^+$	pMD1230	A232	c-myc
A2758	multicopy Ste2p(Δ305−431)[b]	*GPA1*$^+$	*STE4*$^+$	pMD1055 + pMD284	A575	c-myc
A2759	multicopy Ste2p(Δ305−431)[b]	*gpa1*-Δ	*STE4*$^+$	pMD1055 + pMD284	A1017	c-myc
A2964	multicopy Ste2p(Δ305−431)[b]	*GPA1*$^+$	*ste4*-Δ	pMD1055 + pMD284	A2951	c-myc
A2739	*ste2*-Δ	*gpa1*-Δ	*STE4*$^+$	pMD228 + pMD284	A1017	
A1686	*ste2*-Δ	*GPA1*$^+$	*STE4*$^+$	pMD228 + pMD284	A575	
A454	*ste2*-Δ	*GPA1*$^+$	*STE4*$^+$	pMD228	A232	
A2966	*ste2*-Δ	*GPA1*$^+$	*ste4*-Δ	pMD228 + pMD284	A2951	

[a] Full-length c-myc-tagged Ste2p containing Asn430 → Ala. [b] Ste2p(Δ305−431) c-myc-tagged containing Cys252 → Ser.

methanol/water (1:1). All experiments used ligand solutions prepared less than 3 h in advance.

The biological activity of [K^7(NBD),Nle^{12}] α-factor was assessed by its ability to induce *FUS1-lacZ* expression in a fluorescent β-galactosidase assay as described previously (*35*). Both the unlabeled and fluorescent α-factor stock solutions for the assay were dissolved in a solution of methanol/water (1:1), and the cells were incubated with the desired ligand concentrations at 30 °C for 105 min in the presence of light.

Fluorescence Microscopy. Yeast cultures expressing the full-length or the truncated receptor were grown to stationary phase and then diluted and cultured overnight to an OD_{600} of approximately 1.0. A total of 10^7 cells were harvested and resuspended in 20 mM ice cold 2-(*N*-morpholino)-ethanesulfonic acid (MES) buffer, pH 5.8, to a final volume of 200 μL. The cells were then incubated with the fluorescent ligand (100 nM [K^7(NBD),Nle^{12}] α-factor) for the desired time period on ice. To study the time course of endocytosis, the same number of cells were harvested and resuspended in synthetic complete medium lacking uracil medium. The cell suspension was incubated with the fluorescent ligand at 30 °C for the indicated time periods. Cell suspensions were examined using a Nikon Diaphot 200 inverted microscope equipped with a CCD camera (Princeton Instruments), a 100× objective with 1.4 NA, and a standard fluorescein isothiocyanate (FITC) filter. Images were analyzed using the program Metamorph from Universal Imaging. The autoscaling feature of Metamorph was used to adjust image intensities in Figures 1 and 2 to a uniform grayscale range, although the ranges of raw image intensities for micrographs of the truncated receptors were approximately twice as great as those for micrographs of the full-length receptors.

Equilibrium Binding Assays. Yeast cultures to be used for binding assays were grown to stationary phase, then diluted, and cultured overnight. When they reached an OD_{600} of 0.75−1.2, a volume of yeast culture corresponding to 1.5×10^6 cells was transferred to polystyrene tubes on ice. Ice-cold 20 mM MES, pH 5.8, was added so that the final volume, including ligand volume (<40 μL), was 500 μL. These samples were incubated with the ligand solutions for 40−80 min on ice, then vortexed briefly before analysis on a Becton and Dickinson FACSCalibur flow cytometer using excitation at 488 nm. Samples were maintained on ice and protected from light during preincubations and flow cytometry analysis.

Mean fluorescence values for a particular batch of yeast cells incubated at various ligand concentrations were corrected for autofluorescence by subtracting the mean fluorescence value obtained for the same culture in the absence of any ligand. Binding data was analyzed using the ligand-binding module of Sigmaplot (SPSS Inc). B_{max} and K_d values were obtained by fitting to a binding equation that allowed for single-site specific binding, as well as a nonspecific component, $Y = B_{max}L/(K_d + L) + NL$, where Y is the mean fluorescence of cells, N is the proportionality constant for nonspecific binding to cells, and L is the ligand concentration in nanomolar. The B_{max} and K_d values obtained were an average of at least three independent experiments using independent yeast transformants.

To determine K_i values for competition with nonfluorescent ligands, cells were incubated with various ratios of [K^7-(NBD),Nle^{12}] α-factor and synthetic unlabeled α-factor (Bachem AG) for 60−100 minutes on ice. IC_{50} values were fit using the one-site competition equation in the ligand-binding module of Sigmaplot. K_i values were calculated using the equation $K_i = IC_{50}/(1 + [\text{labeled ligand}]/K_d)$, using K_d values determined for the labeled ligand from saturation binding experiments for the particular strains being studied. The presented values obtained were an average of at least three independent experiments.

Assays of Binding Kinetics. Cell cultures and ligand solutions were prepared as described above. A volume of ice-cold 20 mM MES, pH 5.8, was added to 3×10^6 cells to make up the final volume to 1000 μL. Ligand was then added, the suspension was vortexed, and data acquisition using the FACSCalibur in lapsed-time mode was begun within approximately 10−15 s after adding the ligand solution. The mean fluorescence values obtained at each time point were corrected for autofluorescence by subtracting the value obtained in the absence of the fluorescent ligand. Samples were maintained on ice and protected from light. The values obtained after subtraction were fitted with a single-exponential association equation $Y = Y_{max}(1 - e^{-K_{obs}t})$,

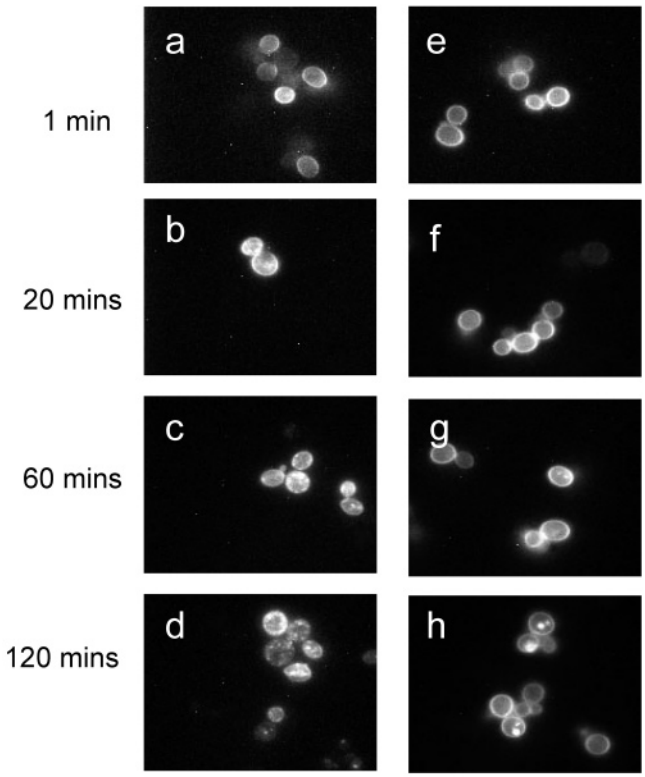

FIGURE 1: Endocytosis of [K^7(NBD),Nle^{12}] α-factor detected with fluorescence microscopy. Cells expressing full-length receptors (left panels) or truncated receptors (right panels) from multicopy plasmids were incubated with the fluorescent ligand at 30 °C for (a,e) 1, (b,f) 20, (c,g) 60, and (d,h) 120 min. The ranges of image intensities in panels e−h are approximately 2-fold greater than those for panels a−d, indicative of stronger fluorescence from the truncated receptors. The strains expressing the full-length and truncated receptors are A2728 and A2912, respectively.

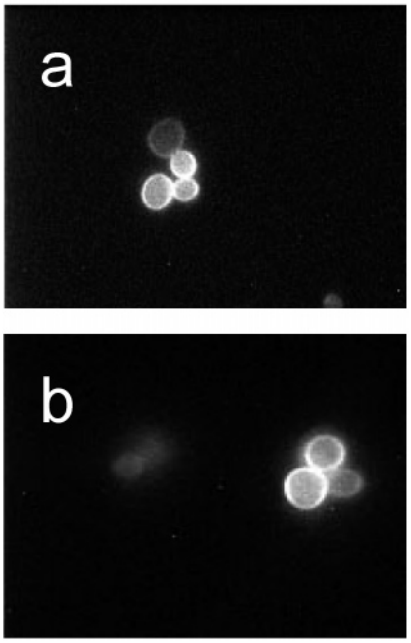

FIGURE 2: Inhibition of [K^7(NBD),Nle^{12}] α-factor internalization visualized under a fluorescence microscope. Cells expressing full-length receptors (a) or truncated receptors (b) from multicopy plasmids were incubated with the fluorescent ligand on ice for 2 h. The strains expressing the full-length and truncated receptors are A2728 and A2912, respectively.

where Y is the mean fluorescence of cells at various time points, Y_{max} is the maximum mean fluorescence value obtained at equilibrium for a particular ligand concentration, K_{obs} expressed in units of s^{-1} is the pseudo-first-order rate constant, and t is the time in seconds for a particular ligand concentration to reach equilibrium. The same data was then fitted to a double-exponential association equation $Y = A(1 - e^{-Bt}) + C(1 - e^{-Dt})$, where A and C are the maximum contributions to the fluorescence for each kinetic component at a particular ligand concentration and B and D are the pseudo-first-order rate constants for the two components.

Global nonlinear least-squares fitting to a two-step sequential binding reaction, L + R ↔ LR ↔ LR*, was conducted using the program Dynafit (*36*). The total concentration of receptors in each experiment was considered as a single adjustable parameter. The response factor for the LR state, a measure of the amount of fluorescent signal per nanomolar of bound ligand in this state, was also considered as an adjustable parameter. However, the response factor of the LR* state was set at 100 fluorescent units/nM. (This was necessary because the response factor and the total concentration of receptors are closely interdependent in the fitting and could not be fit independently). The fit to the two-step reaction for the C-terminal-truncated receptor yielded a best-fit overall concentration of receptors of 0.32 ± 0.001 nM and a response factor for the LR state of 137 ± 8 units/nM (i.e., 1.4 times greater fluorescence intensity per nanomolar than the LR* state). For full-length receptors, the best-fit overall concentration of receptors was 0.15 ± 0.01 nM, and the response factor for the LR state was 0.46 ± 0.04 times the response factor for the LR* state. While this lower fluorescence for the LR state compared with the LR* state might appear to indicate that the initial location of ligand bound to full-length receptors is less hydrophobic than the final location in the LR* state, the significance of this difference is not clear, given the relatively poor fit of binding kinetics for the full-length receptor (see below) and the fact that time-dependent changes in fluorescence emission spectrum indicate that the initial location is more hydrophobic than the final location (see below).

To accurately quantitate the concentrations of ligand in the binding rate determinations in view of uncertainties in determining and maintaining low concentrations of ligand in solution, the concentrations of α-factor used in the global fitting (for values below 100 nM) were determined based on equilibrium fluorescence levels, as follows: The maximal level of fluorescence achieved at long incubation times for each kinetic dataset was determined from the fit to a single-exponential rate equation, and the maximal level of fluorescence (Y_{max}, see above) was taken as an equilibrium level of fluorescence. The concentration of ligand corresponding to this level of fluorescence was then calculated from the equilibrium binding parameters for the relevant strain listed in Table 3. In cases where there were variations in the Y_{max} values obtained for different determinations of binding kinetics, datasets with Y_{max} values closest to the expected values derived from equilibrium binding assays were selected for further analysis. To reduce possible complications in the binding kinetics resulting from nonspecific binding, the maximum ligand concentration used in characterization of the binding to full-length receptor was 80 nM. At this

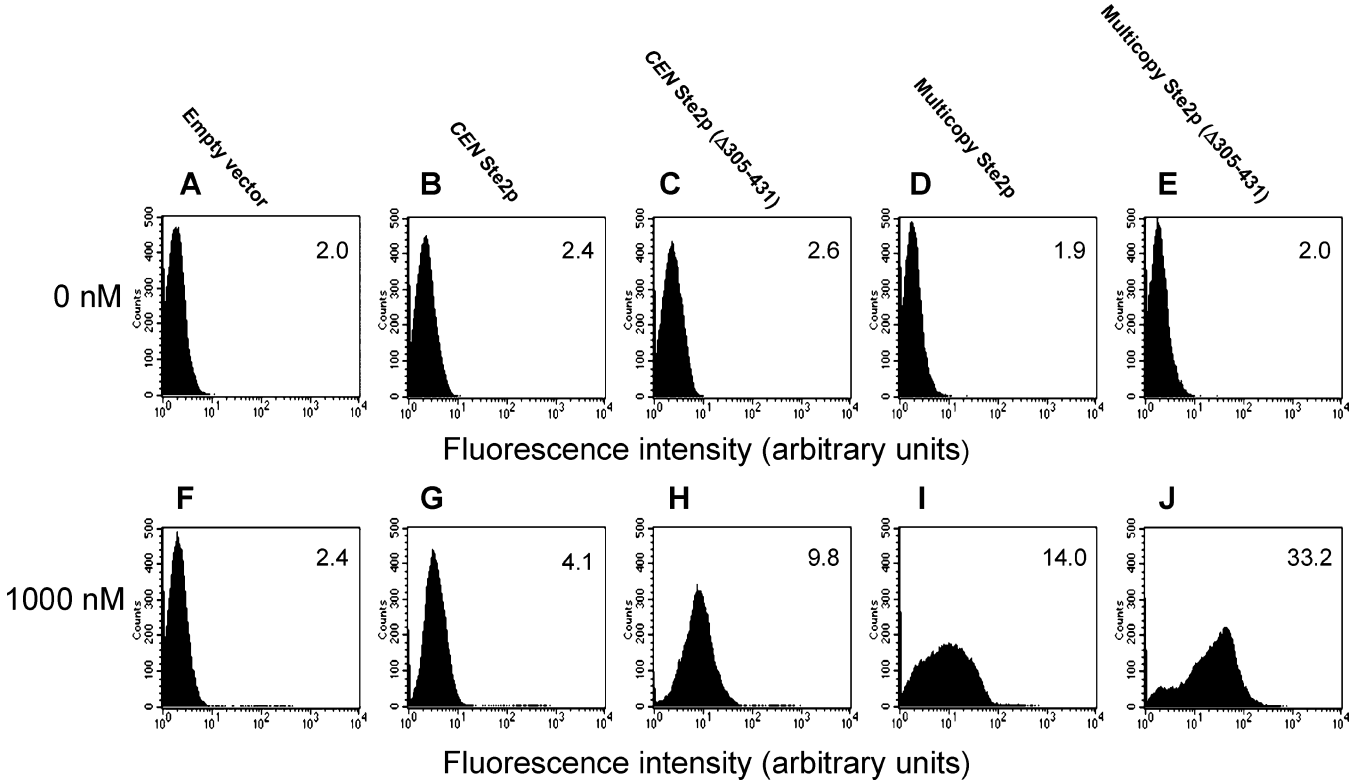

FIGURE 3: FACS histograms of cells expressing no receptors (A,F), full-length receptors from a *CEN* plasmid (B,G), truncated receptors from a *CEN* plasmid (C,H), full-length receptors from a multicopy plasmid (D,I), truncated receptors from a multicopy plasmid (E,J) in the absence (top panels) and presence of a saturating concentration of the ligand (bottom panels). The histograms represent data obtained for at least three independent experiments. The strains expressing the full-length or truncated receptors from *CEN* plasmids are A2933 and A2927, respectively. The strains expressing receptors from multicopy plasmids are the same as those used in Figures 1 and 2. The strain expressing no receptor is A454.

concentration, the contribution of nonspecific binding is less than 2% of the equilibrium level of mean fluorescence.

The ratio of mean fluorescence in the FL1 and FL2 channels of the flow cytometer (FL1/FL2) was corrected for autofluorescence as follows: The mean fluorescence in each channel was determined for each particular culture of yeast cells in the absence of the fluorescent ligand. This value was then subtracted from the mean fluorescence in the same channel in the presence of various concentrations of the ligand at various times before calculating the channel ratio.

RESULTS

Fluorescence Microscopy of [K^7(NBD),Nle^{12}] α-Factor Binding to Cells. As an initial test of the ability to detect receptor-bound [K^7(NBD),Nle^{12}] α-factor and to determine the effects of ligand internalization on binding assays, we used epifluorescence microscopy to examine the distributions of ligand in the presence of cells. Although previous studies have documented the subcellular distribution of receptors, either fused to green fluorescent protein (*37*) or using indirect immunofluorescence (*38*), the use of fluorescent [K^7(NBD),-Nle^{12}] α-factor allows direct visualization of the subcellular distribution of ligand as a function of time. Within seconds after adding [K^7(NBD),Nle^{12}] α-factor to cells, we detected an increase in fluorescence associated with the surface of cells expressing receptors (Figure 1a,e) but no corresponding increase in cells containing a deletion of the *STE2* gene encoding the α-factor receptor (results not shown). The increased fluorescence was very strong in cells expressing truncated receptors lacking the cytoplasmic C-terminal tail (Figure 1e−h), as expected from previous studies demonstrating that this truncation greatly increases the number of cell-surface binding sites (*39*, *40*). The increased fluorescence was also strongly evident in cells containing the full-length *STE2* gene on a multicopy plasmid (Figure 1a−d) but was barely detectable in cells expressing full-length receptors from a single chromosomal copy of *STE2* (data not shown; note that the grayscales of the images in Figures 1 and 2 have been adjusted for visibility as described in Experimental Procedures).

Time-dependent redistribution of fluorescence of [K^7-(NBD),Nle^{12}] α-factor bound to cells was also different in cells expressing full-length compared with truncated receptors. Cells expressing C-terminal-truncated receptors exhibited a uniform distribution of fluorescence at the cell periphery (Figure 1e−h) that was generally maintained even after 2 h of incubation in glucose-containing medium at 30 °C, although large clusters of fluorescent materials eventually appeared inside of some cells. In contrast, a strain expressing full-length receptors accumulated smaller clusters of fluorescent material inside cells after 20 min of incubation with the ligand, with further intracellular accumulations visible after longer incubations (Figure 1a−d).

As described previously (*41*), the combination of low temperature and transfer to a buffer solution lacking a metabolizable energy source effectively blocked internalization (Figure 2). Thus, the ligand-binding assays described below were conducted with cells maintained at 0 °C in the

absence of metabolic inhibitors, the mildest conditions we found that effectively blocked internalization of receptors. No fluorescence on the cell periphery or in internal compartments was visible when micrographs of *ste2*-Δ cells were visualized at the same imaging and scaling settings used for Figures 1 and 2. Under conditions where endocytosis is not expected to be rapid (i.e., using cells expressing truncated receptors or in short incubations with cells expressing full-length receptors), no significant difference was detected between binding assays conducted at room temperature compared with 0 °C.

Equilibrium Binding of α-Factor Assayed by Flow Cytometry. In the flow cytometer, cells traversing a narrow channel pass through a laser beam focused on a small volume of suspension. The presence of cells is detected by light scattering, allowing fluorescence intensities to be recorded only when the instrument detects a cell passing through the illuminated volume, thereby eliminating most background fluorescence from unbound ligand in solution. Thus, the amount of ligand associated with cells can be assessed in an equilibrium experiment. Sensitivity is enhanced by the use of a ligand like [K^7(NBD),Nle^{12}] α-factor that exhibits an increase in fluorescence emission upon binding receptor (*18*).

It is evident from the histograms shown in Figure 3e,j that in the presence of [K^7(NBD),Nle^{12}] α-factor most cells expressing truncated receptors exhibited a shift to higher fluorescence levels. This was also true for cells expressing full-length receptors encoded on a multicopy plasmid (Figure 3d,i). Cells expressing full-length receptors from a *CEN* plasmid exhibited a shift in mean fluorescence that was not obvious by visual inspection of the histograms but was detectable and reproducible based on changes in calculated mean fluorescence (Figure 3b,g). Cells containing no *STE2* gene exhibit minimal shifts in mean fluorescence in the presence of [K^7(NBD),Nle^{12}] α-factor (Figure 3a,f) indicative of the insensitivity of the assay to nonspecific binding. Even at a ligand concentration of 1 μM, the increase in mean fluorescence of receptor-less cells was only 3% of the maximum equilibrium fluorescence of cells expressing the (multicopy) full-length Ste2p and 1% of the maximum fluorescence of the cells expressing (multicopy) truncated receptors.

As shown in Figure 3, yeast cells exhibit significant autofluorescence in the absence of ligand. Because we find that autofluorescence varies slightly from yeast strain to yeast strain and depends on growth conditions, we applied specific corrections for autofluorescence to each batch of cells studied based on the fluorescence of the particular batch of cells in the absence of added ligand. Nonspecific binding of ligand also appeared to vary with the particular batch of cells, so a correction for nonspecific binding was determined for each culture from nonlinear least-squares fitting of mean fluorescence to a binding equation that includes a term for nonspecific binding (see Experimental Procedures). Since we do not know the exact fluorescence emission per molecule of bound [K^7(NBD),Nle^{12}] α-factor, the B_{max} values are presented as relative fluorescence units per cell. To ensure that the results of binding assays were not affected by depletion of the ligand, we compared the results of binding assays conducted using the normal cell count of 3×10^6 cells/mL with similar assays conducted at 1×10^6 and 0.6×10^6 cells/mL. These variations in cell density did not result in any significant difference in the observed binding parameters (results not shown).

In some cases, binding of fluorescent ligand gave rise to a bimodal histogram of fluorescence intensities of cells. This type of distribution was observed for cells at a wide variety of different growth stages and for cells that either had or had not been pretreated with α-factor. Since each yeast culture was derived from a single colony, it is unlikely that the distribution can be explained by spontaneous generation of genetic diversity among the cells. The bimodal distribution was observed for cells expressing receptors from multicopy plasmids, which should be present at a gene dosage of ~50 copies per cell, leading to expression of at least thousands of receptors per cell (*40*, *42*), making it unlikely that such a distribution could be due to random statistical fluctuations in levels of receptor expression. A similar bimodal distribution has been observed for α-factor receptors fused to green fluorescent protein (results not shown) and for other proteins expressed in yeast (*23*). The most likely explanation for the two populations of cells appears to be an all-or-none regulation of *STE2* expression, as has been reported for other transcriptional systems in yeast (*43*). This means that in assays in which we monitor changes in mean fluorescence, we are actually tracking changes only in the receptor-expressing population of cells, which is expected to be a constant proportion of any particular cell culture.

Binding of [K^7(NBD),Nle^{12}] α-factor to yeast cells is effectively competed by normal nonfluorescent synthetic α-factor (Figure 4). The IC_{50} and K_i values listed in Table 2 for the competition of [K^7(NBD),Nle^{12}] α-factor by unlabeled α-factor are consistent with published values for the dissociation constant of unlabeled α-factor (*12*). We have also confirmed that the biological activity of [K^7(NBD),Nle^{12}] α-factor is similar to that of the unlabeled pheromone in a quantitative liquid assay of *FUS1-lacZ* induction (Figure 5). Previously, halo assays of pheromone-induced growth arrest of yeast cells in response to [K^7(NBD),Nle^{12}] α-factor had indicated that the fluorescent ligand exhibited reduced signaling activity (*18*). Differences observed in comparing *FUS1-lacZ* induction to the halo assay in response to the different ligands most likely reflect differences in the stability or solubility of ligand in the short-term liquid β-galactosidase assay compared with the long-term plate-based halo assay.

We used the fluorescence-based assay to reexamine equilibrium binding of ligand to various yeast strains (Figure 6 and Table 3), addressing the following issues:

1. Effects of Variations in Copy Number and of C-Terminal Truncation of Receptor. The number of binding sites for [K^7-(NBD),Nle^{12}] α-factor in strains expressing the truncated receptor from a multicopy plasmid was 2−3 times higher than for cells expressing multiple copies of a similarly tagged full-length Ste2p (Table 3). This is a somewhat smaller increase than was seen in previous studies documenting the role of the C-terminal tail in internalization of receptors (*39*, *40*). The dissociation constants of the two types of receptors for [K^7(NBD),Nle^{12}] α-factor determined from equilibrium binding titrations were similar (Table 3), both somewhat lower than the 26.8 nM K_i determined previously (*18*). This difference can be attributed to the fact that the previous experiment was conducted as a competition with radiolabeled α-factor, using a different receptor allele expressed in a different strain background. Only minor variations in affini-

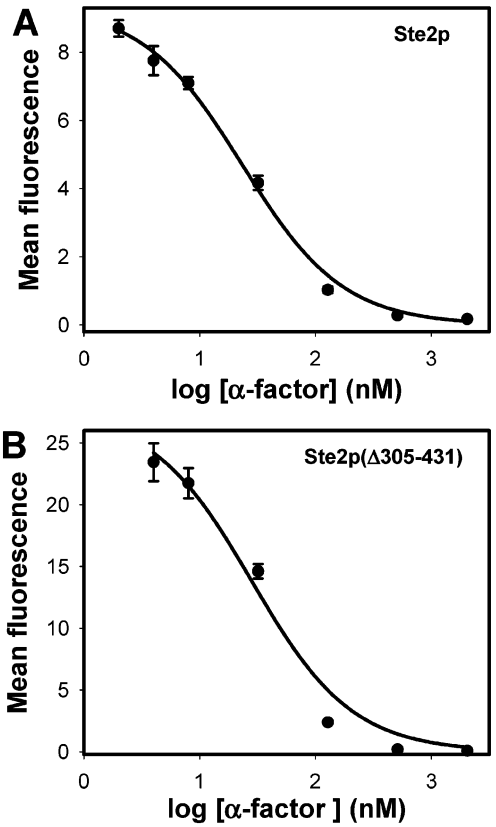

FIGURE 4: Competition by synthetic unlabeled α-factor for binding of 20 nM [K[7](NBD),Nle[12]] α-factor to full-length receptors expressed in strain A2728 (A), and to truncated receptors expressed in strain A2912 (B). Both receptor alleles were expressed from multicopy plasmids. The data plotted is an average of at least three independent experiments.

Table 2: IC_{50} and K_i Values for Agonist Binding to Full-Length and Truncated Receptors[a]

STE2 allele	IC_{50} (α-factor) (nM)	K_i (α-factor) (nM)	yeast strain
Ste2p[b]	23.4 ± 1.7	6.4 ± 1.5	A2728
Ste2p(Δ305−431)	27.9 ± 1.8	9.5 ± 2.5	A2912

[a] IC_{50} and K_i values are expressed as mean ± SEM of at least three independent experiments. [b] Full-length c-myc-tagged Ste2p containing Asn430 → Ala.

ties of various receptor alleles for [K[7](NBD),Nle[12]] α-factor were detected along with the differences in abundance.

2. Effects of Varying the Receptor−G Protein Ratios. Some GPCRs exhibit higher affinities for ligand when they are coupled to G proteins, presumably because the interaction with G protein stabilizes an active state of the receptor (see ref *44*). In the case of the α-factor receptor, it has been reported that membranes derived from cells carrying mutant G protein subunits exhibit reduced affinity for α-factor compared with normal membranes. This decrease in affinity also takes place upon treatment of normal membranes with GTPγS (*45*). The α-factor receptor and G protein heterotrimer may also exist in a nonsignaling "preactivation" complex involving the cytoplasmic C-terminal tail of the receptor, since truncation of the tail renders ligand binding insensitive to GTPγS in isolated membranes and abrogates dominant negative effects of certain mutant alleles (*42*).

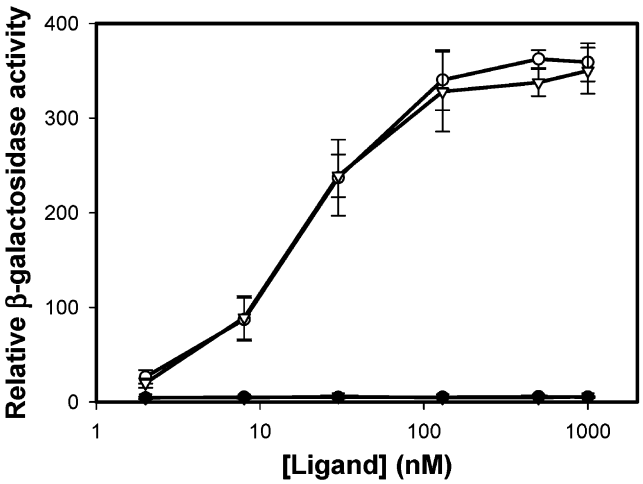

FIGURE 5: Comparison of biological activity of [K[7](NBD),Nle[12]] α-factor (▽) and a synthetic unlabeled α-factor (○) in a *β*-galactosidase assay using cells expressing no receptor (closed symbols) and cells expressing the full-length receptors on a multicopy plasmid (open symbols). The empty vector and the full-length receptor strains are the same as those used in Figure 3. The error bars represent standard error.

We compared binding of fluorescent ligand to various receptor alleles in cells expressing the normal chromosomal complement of G protein subunits with binding to cells completely lacking the G_α subunit because of a chromosomal deletion of the *GPA1* gene (Table 4). Full-length receptors expressed from multicopy plasmids exhibit a 2-fold higher affinity and truncated receptors expressed from multicopy plasmids exhibit an 8-fold increase in affinity in cells lacking Gpa1p ($p < 0.05$). In contrast, no significant difference in affinity was associated with deletion of *GPA1* for full-length receptors expressed from *CEN* plasmids. *MAT***a** yeast strains that fail to express *GPA1* exhibit constitutive activation of the pheromone pathway leading to altered growth and morphology, even in a *far*-Δ host that should be resistant to pheromone response-activated cell cycle arrest (*24*). This makes it difficult to interpret the apparent reductions in levels of cell-surface expression of full-length or truncated receptors associated with deletion of *GPA1*. However, these considerations should not affect the measurement of ligand affinities. Furthermore, a similar increase in affinity was observed for truncated receptors in a strain lacking *STE4*, encoding the G_β subunit, which should not be subject to altered growth and morphology (results not shown). (Because of low levels of receptor expression in *ste4*-Δ strains (*45*), it was only possible to reliably determine receptor affinity in the *ste4*-Δ strain expressing truncated receptors.)

Binding Kinetics. Following approaches used previously by Sklar and colleagues (*21*, *46*), we conducted a series of experiments in which various concentrations of the fluorescent ligand were rapidly mixed with cells expressing truncated (Figure 7) and full-length (Figure 8) receptors, then subjected to time-resolved flow cytometry. The time course of fluorescence changes in these experiments was initially fit to single-exponential binding kinetics that would be expected for binding of a single class of ligands to a single class of binding sites in a single-step reaction. However, the nonlinear least-squares fits obtained at various concentrations displayed systematic deviations from single-exponential kinetics (see Figures 7 and 8), and the best-fit rate constants

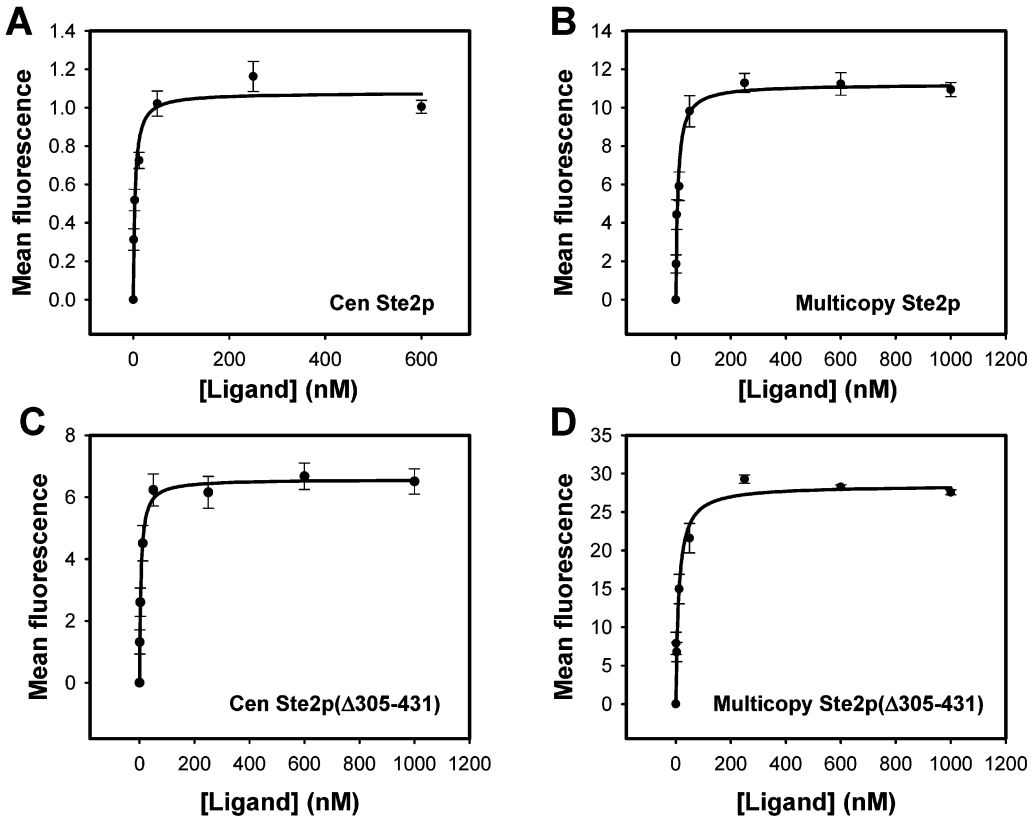

FIGURE 6: Saturation binding of [K[7](NBD),Nle[12]] α-factor to full-length receptors expressed from a *CEN* plasmid in strain A2933 (A), to full-length receptors expressed from a multicopy plasmid in strain A2728 (B), to truncated receptors expressed from a *CEN* plasmid in strain A2927 (C), and to truncated receptors expressed from a multicopy plasmid in strain A2912 (D). The data plotted is an average of at least three independent experiments.

Table 3: B_{max} and K_d Values for Full-Length and Truncated Receptors Expressed from *CEN* and Multicopy Plasmids in Cells Containing a Normal Chromosomal *GPA1* Locus

STE2 allele	epitope	B_{max}[c]	K_d[c] (nM)	yeast strain
CEN Ste2p[a]	c-myc	1.1 ± 0.1	3.7 ± 0.8	A2933
multicopy Ste2p[a]	c-myc	11.2 ± 0.4	7.6 ± 1.7	A2728
CEN Ste2p(Δ305−431)	c-myc	6.6 ± 0.4	5.3 ± 1.9	A2927
multicopy Ste2p(Δ305−431)	c-myc	28.5 ± 0.2	11 ± 3.5	A2912
multicopy Ste2p(Δ305−431)[b]	c-myc	33.1 ± 0.8	8.5 ± 1.2	A2662

[a] Full-length c-myc-tagged Ste2p containing Asn430 → Ala. [b] Ste2p(Δ305−431) c-myc-tagged containing Cys252 → Ser. [c] B_{max} and K_d values are expressed as mean ± SEM of at least three independent experiments.

Table 4: Equilibrium Binding Parameters of *GPA1*$^+$ and *gpa1*-Δ Strains

GPA1 allele	B_{max}[a]	K_d[a] (nM)	yeast strain
	Full-Length Ste2p (Multicopy)		
GPA1$^+$	19.7 ± 0.5	7.2 ± 1.4	A2735
gpa1-Δ	3.9 ± 0.9	3.5 ± 0.5	A2733
	Ste2p(Δ305−431) (Multicopy)		
GPA1$^+$	24.8 ± 2.7	15.9 ± 1.6	A2758
gpa1-Δ	21.8 ± 3.9	1.9 ± 0.3	A2759
	Full-Length Ste2p (*CEN*)		
GPA1$^+$	0.6 ± 0.2	3.5 ± 0.8	A2737
gpa1-Δ	1.9 ±0.2	4.8 ± 1.1	A2738

[a] B_{max} and K_d values are expressed as mean ± SEM of at least three independent experiments.

did not exhibit the expected linear dependence on ligand concentration (results not shown). At every concentration tested, the use of two exponentials (see Experimental Procedures) yielded a significantly better fit to the data than the single exponential ($p < 10^{-9}$, using the *f* test) (Table 5). In general, we observed a slower kinetic phase that varied with ligand concentration, and a faster phase that was relatively independent of ligand concentration.

Although the multiexponential kinetics of binding could, in principle, be indicative of two simultaneous but distinct binding events, the equilibrium binding data provided no evidence for multiple classes of ligands or binding sites. Thus, the observation of multiexponential kinetics is more likely to reflect a multistep binding reaction in which a second-order binding reaction is followed by a conversion of the ligand−receptor complex to an activated state. The program Dynafit (*36*) was used to perform global nonlinear least-squares fits of the kinetics of binding at different ligand concentrations to the differential equations describing the reaction:

$$L + R \underset{k_{off}}{\overset{k_{on}}{\leftrightarrow}} LR \underset{k_2}{\overset{k_1}{\leftrightarrow}} LR^*$$

The global fits to the kinetics of binding to full-length and truncated receptors at different ligand concentrations shown in Table 6 are consistent with an initial binding rate comparable to that observed previously using a time-resolved filtration assay with radiolabeled ligand (*12*, *14*), which is slower than expected for a diffusion-controlled reaction. The values of k_1 derived from the fitting indicate that the second step of the reaction, conversion to the activated complex,

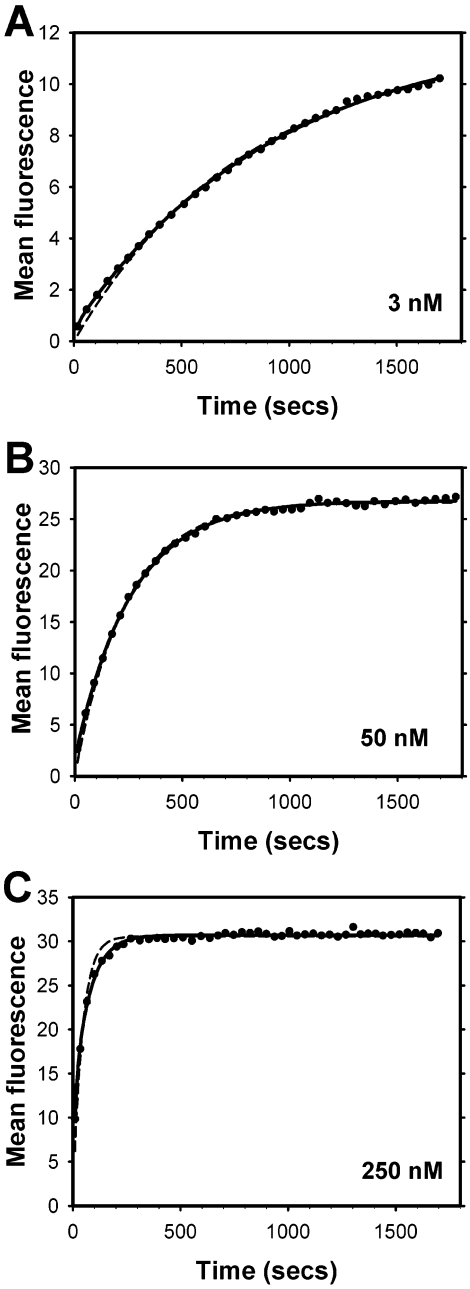

FIGURE 7: Kinetics of binding of [K^7(NBD),Nle^{12}] α-factor to cells of strain A2662 expressing truncated receptors from a multicopy plasmid fitted using a single-exponential association equation (− − −) and a double-exponential association equation (—) at (A) 3, (B) 50, and (C) 250 nM.

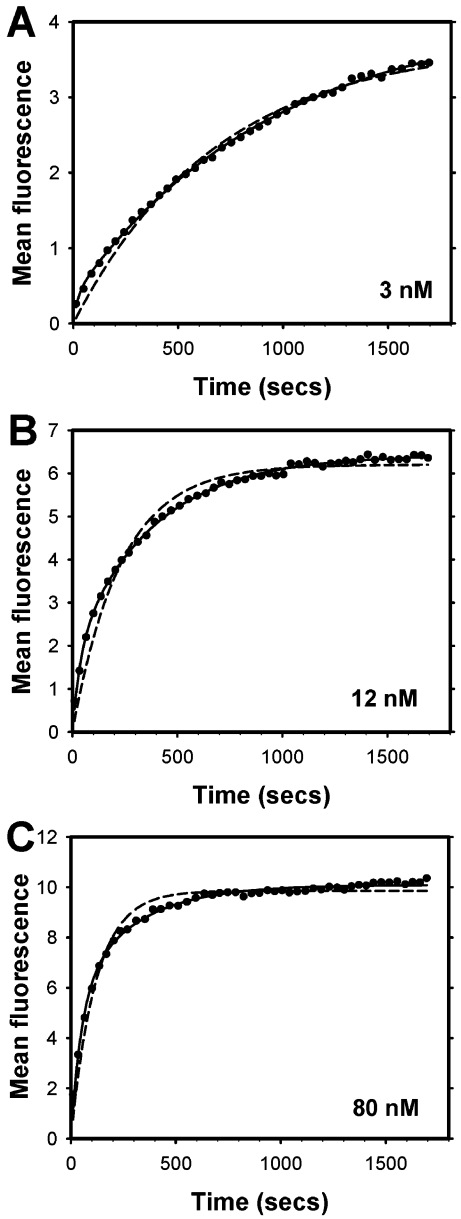

FIGURE 8: Kinetics of binding of [K^7(NBD),Nle^{12}] α-factor to cells of strain A2728 expressing full-length receptors from a multicopy plasmid fitted using a single-exponential association equation (− − −) and a double-exponential association equation (—) at (A) 3, (B) 12, and (C) 80 nM.

takes place on a time scale of 0.5−5 min. The fits to the two-stage process, determined from the global least-squares fitting to the relevant differential equations, were significantly better than similar fits to single-stage kinetics (not shown) ($p < 0.01$). Attempts to fit the second step of the reaction to a second-order process involving association of the LR complex with either unoccupied receptors or a second LR complex provided no significant improvement to the fitting. The fit shown in Figure 9 for the full-length receptor was not as good as that for the truncated receptor, presumably because of lower signal strengths.

To date, we have been unable to measure the dissociation kinetics for the interaction of [K^7(NBD),Nle^{12}] α-factor with cells, either by diluting the added ligand or by adding large excesses of unlabeled α-factor either on ice or at room temperature. This is true even under conditions where the ligand was incubated with cells only for a short period. This may, in part, be the result of a slow off-rate resulting from the two slow steps of dissociation (Table 6). The observed low level of association of fluorescent ligand with cells lacking receptors rules out the possibility that the apparent slow off-rate results from any nonspecific association of ligand with membranes.

The emission maximum of [K^7(NBD),Nle^{12}] α-factor shifts from 545 nm in aqueous solution to 530 nm (accompanied by a large increase in fluorescence) in the hydrophobic environment of 90% dioxane (*18*). This raised the possibility of examining the relative polarity of the LR state in comparison to the LR* state based on the time-resolved measurements of the emission spectrum. The FACSCalibur

Table 5: Parametric Values Obtained by Fitting the Kinetic Data Obtained at Various Concentrations of [K[7](NBD),Nle[12]] α-Factor to a Single- (K_{obs} and Y_{max}) and a Double-Exponential Association Equation (A, B, C, D)[a]

concentration (nM)	K_{obs}	Y_{max}	A	B	C	D
			Ste2p(Δ305−431) (Multicopy)			
3	1.2	11.5	0.53	71.3	11.6	1.1
12	2.8	24.2	12.1	5.9	14.3	1.2
50	4.2	26.6	1.8	148	25.0	3.8
250	23.6	30.6	11.1	110	19.6	13.9
600	87.1	32.1	26.0	129	6.2	15.1
			Full-Length Ste2p (Multicopy)			
3	1.5	3.7	0.36	46.9	3.7	1.1
12	4.3	6.2	1.8	26.4	4.6	2.7
40	4.6	8.9	2.9	26.1	6.33	2.6
50	5.1	8.3	3.5	15.5	5.1	2.7
80	8.4	9.9	5.6	20.0	4.5	3.5

[a] The receptor-expressing yeast strains used were A2662 (expressing Ste2p(Δ305−431) from a multicopy plasmid) and A2728 (expressing full-length Ste2p from a multicopy plasmid). Y_{max} and K_{obs} refer to the equation $Y = Y_{max}(1 - e^{-K_{obs}t})$. A, B, C, and D refer to the equation $Y = A(1 - e^{-Bt}) + C(1 - e^{-Dt})$. Y_{max}, A, and C have units of mean fluorescence units per cell; K_{obs}, B, and D have units of $s^{-1} \times 10^{-3}$.

Table 6: Parametric Values Obtained from Globally Fitting the Kinetic Data for Binding of [K[7](NBD),Nle[12]] α-Factor to C-Terminal-Truncated and Full-Length Receptors Expressed from Multicopy Plasmids in Strains A2662 and A2728, Respectively[a]

Reaction Mechanism: L + R ⇔ LR (Ste2p(Δ305−431) (Multicopy))

k_{on} (M^{-1} s^{-1})	k_{off} (s^{-1})
$7.2 \times 10^4 \pm 1 \times 10^3$	$9.1 \times 10^{-4} \pm 4 \times 10^{-5}$

Reaction Mechanism: L + R ⇔ LR ⇔ LR* (Ste2p(Δ305−431) (Multicopy))

k_{on} (M^{-1} s^{-1})	k_{off} (s^{-1})	k_1 (s^{-1})	k_2 (s^{-1})
$1.3 \times 10^5 \pm 8 \times 10^3$	$4.4 \times 10^{-2} \pm 6 \times 10^{-3}$	$3.5 \times 10^{-2} \pm 5 \times 10^{-3}$	$1.2 \times 10^{-3} \pm 7 \times 10^{-5}$

Reaction Mechanism: L + R ⇔ LR (Full-Length Ste2p (Multicopy))

k_{on} (M^{-1} s^{-1})	k_{off} (s^{-1})
$1.6 \times 10^5 \pm 4 \times 10^3$	$1.1 \times 10^{-3} \pm 6 \times 10^{-5}$

Reaction Mechanism: L + R ⇔ LR ⇔ LR* (Full-Length Ste2p (Multicopy))

k_{on} (M^{-1} s^{-1})	k_{off} (s^{-1})	k_1 (s^{-1})	k_2 (s^{-1})
$5.2 \times 10^5 \pm 7 \times 10^4$	$1.0 \times 10^{-2} \pm 3 \times 10^{-3}$	$2.9 \times 10^{-3} \pm 6 \times 10^{-4}$	$1.8 \times 10^{-3} \pm 1 \times 10^{-4}$

[a] The data obtained at multiple concentrations of [K[7](NBD),Nle[12]] α-factor were fit to a single-step and a two-step sequential binding reaction using the program Dynafit (*36*) (see text and Figure 9). The indicated errors are derived from the least-squares fitting.

instrument provides two fluorescence detection channels in this wavelength range, channel FL1 (515−545 nm) and channel FL2 (565−605 nm). Thus, the emission shift of [K[7]-(NBD),Nle[12]] α-factor on transfer to a nonpolar environment would be expected to increase the signal collected in FL1

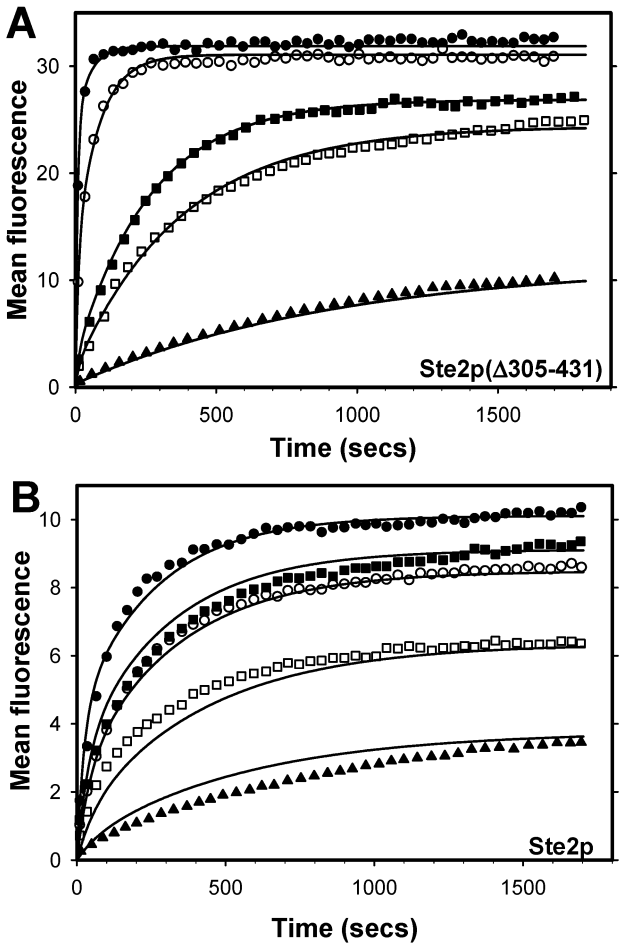

FIGURE 9: Global fitting of the two-step kinetics of binding of [K[7]-(NBD),Nle[12]] α-factor to cells of strain A2662 expressing truncated receptors (A) and strain A2728 expressing full-length receptors (B) from multicopy plasmids using the program Dynafit.

Table 7: Channel Ratios of [K[7](NBD),Nle[12]] α-Factor and [Orn[7](NBD),Nle[12]] α-Factor Bound to Full-Length and Truncated Receptors

STE2 allele	mean fluorescence (channel FL1/channel FL2) [K[7](NBD),Nle[12]]	[Orn[7](NBD),Nle[12]]	yeast strain
Ste2p[a]	2.34 ± 0.01	1.21 ± 0.001	A2728
Ste2p(Δ305−431)	2.20 ± 0.02	1.15 ± 0.004	A2912

[a] Full-length c-myc-tagged Ste2p containing Asn430 → Ala. The ratios are expressed as mean ± SEM of at least three independent experiments.

and decrease the intensity in FL2. As a test of such measurements, we compared the channel ratio for [K[7]-(NBD),Nle[12]] α-factor bound to cells with the ratio for the α-factor analogue [Orn[7](NBD),Nle[12]] α-factor. The NBD fluorophore in [Orn[7](NBD),Nle[12]] α-factor bound to receptors has previously been reported to occupy a relatively hydrophilic environment compared to its environment in [K[7]-(NBD),Nle[12]] α-factor by virtue of being one methyl group closer to the peptide backbone of the ligand (*18*). Consistent with this previous study, we find that the channel ratio (FL1/FL2) for fluorescence of a saturating concentration of [K[7]-(NBD),Nle[12]] α-factor bound to truncated receptors is 2.20, whereas the comparable ratio for the α-factor homologue [Orn[7](NBD),Nle[12]] α-factor is 1.15 (Table 7).

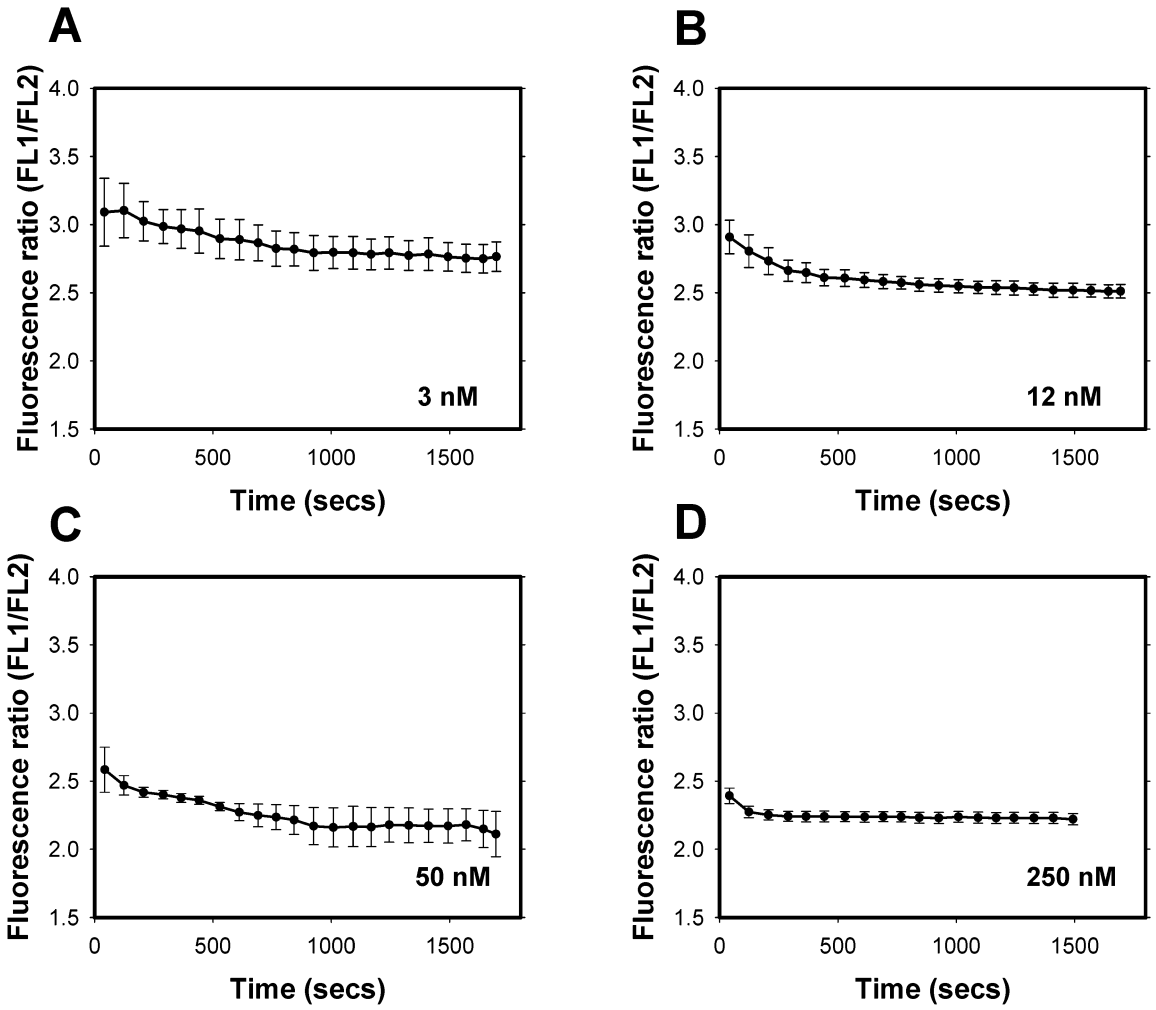

FIGURE 10: Kinetics of channel ratio change for [K^7(NBD),Nle^{12}] α-factor binding to cells of strain A2662 expressing truncated receptors from a multicopy plasmid at total ligand concentrations of (A) 3, (B) 12, (C) 50, and (D) 250 nM. At each concentration the ratios are an average of data obtained for three independent experiments. The error bars represent standard error.

During the interaction of [K^7(NBD),Nle^{12}] α-factor with cells expressing either truncated (Figure 10) or full-length (Figure 11) receptors, the ratio of the emission in channel FL1 to that in channel FL2 undergoes a time-dependent decrease, indicative of a shift in the emission maximum to longer wavelengths and transfer from a hydrophobic to a more polar environment. Such a shift is in the opposite direction from that observed for overall binding of [K^7-(NBD),Nle^{12}] α-factor to receptors (*18*). The simplest explanation for this time-dependent shift is that it corresponds to a second kinetic transition of bound ligand, indicative of transfer from an initial hydrophobic environment to a more polar environment. The rate of change of fluorescence in the second step of the binding reaction, as outlined in the above reaction scheme, should be independent of ligand concentration. However, the rates reflected by the traces in Figures 10 and 11 are a mixture of the first and second steps of the reaction, making it difficult to separate the components.

At low ligand concentrations, unbound or nonspecifically bound ligand is not expected to contribute significantly to the fluorescence channel ratio, given the low fluorescence emission of the ligand in solution, the selectivity of the flow cytometer for cell-associated fluorescence, and the low nonspecific binding detected in equilibrium experiments. However, a small time-independent contribution from unbound or nonspecifically bound ligand provides an explanation for the decrease in the final values of the channel ratios that was observed at high ligand concentrations in Figures 10 and 11. Such low channel ratios, indicative of a more polar fluorophore environment, may reflect an increasing contribution from the fluorescence of unbound ligand present when the overall ligand concentration is much higher than the dissociation constant for binding. The variations in final channel ratio are observed in incubations for times as long as 90 min and, thus, are not due to the failure to reach equilibrium during the time courses indicated in Figures 10 and 11 (results not shown).

DISCUSSION

We report here the use of fluorescence microscopy and flow cytometry to characterize the binding of the fluorescent agonist, [K^7(NBD),Nle^{12}] α-factor, to Ste2p, the yeast α-factor receptor. Distributions of ligand visualized on receptor-expressing cells by fluorescence microscopy vary depending on the particular expressed receptor allele. Internalization of ligand bound to full-length (but not truncated) receptors resulted in the appearance of intracellular fluorescent clusters. This provides direct visual confirmation of

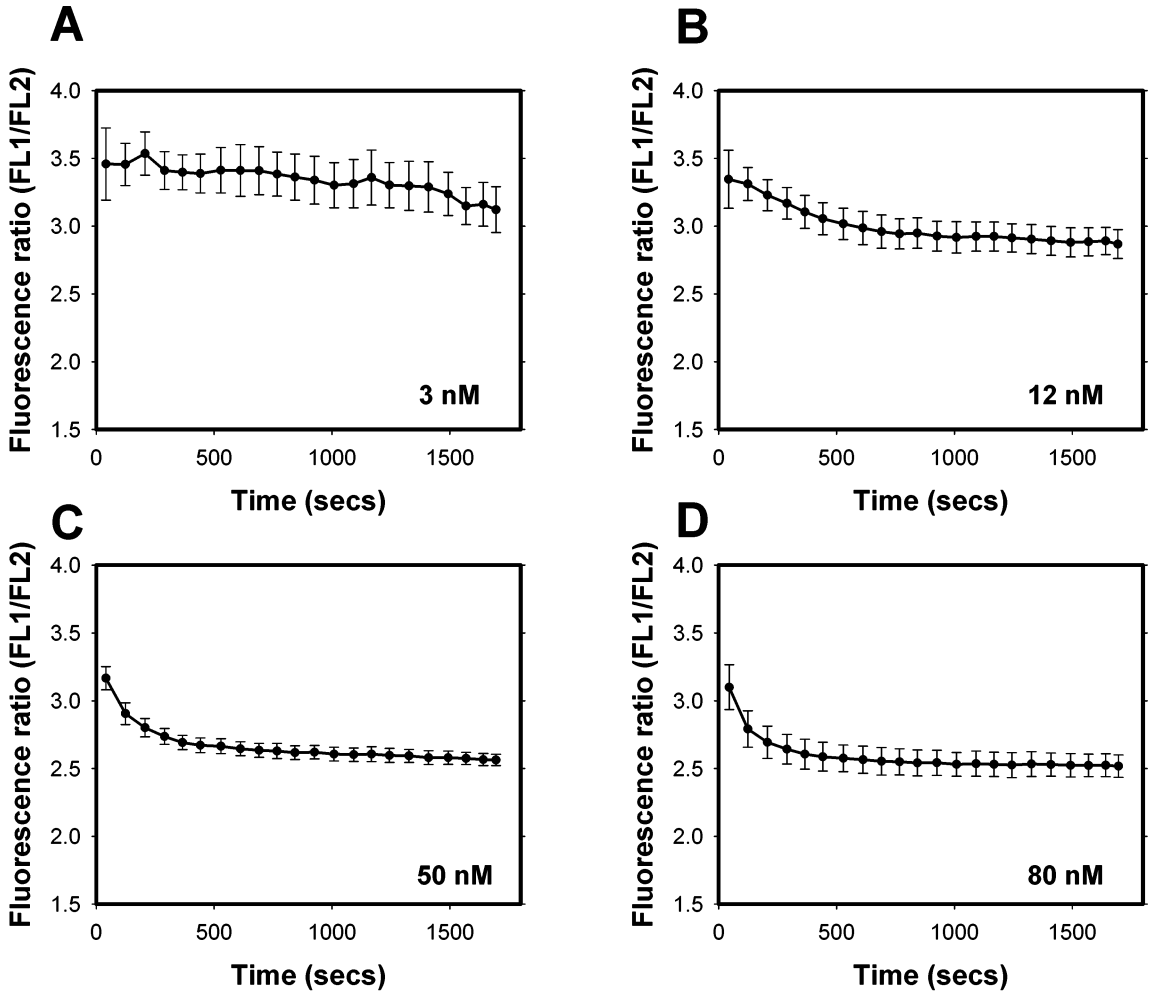

FIGURE 11: Kinetics of channel ratio change for [K^7(NBD),Nle^{12}] α-factor binding to cells of strain A2728 expressing full-length receptors from a multicopy plasmid at total ligand concentrations of (A) 3, (B) 12, (C) 50, and (D) 80 nM. At each concentration the ratios are an average of data obtained for three independent experiments. The error bars represent standard error.

previous studies indicating that α-factor is internalized as a complex with its receptor (*37*, *47*). Maintenance of cells on ice in the absence of energy sources was sufficient to prevent internalization on the time scale necessary for conducting binding assays.

The assay of [K^7(NBD),Nle^{12}] α-factor binding to cells using a flow cytometer provides sufficient sensitivity for detection of binding to receptors expressed in single copy, though binding parameters are better determined using cells with increased receptor expression. The assay is very reproducible and has the following advantages over previous procedures using radiolabeled ligand: (1) The ligand is stable. (2) Assays are conducted at equilibrium, eliminating the need for washing steps that can affect the measurement of equilibrium and kinetic binding constants. (3) When receptors are expressed at adequate levels, the contribution of nonspecific binding to cell-associated fluorescence is low, allowing the assay to be conducted at high ligand concentrations. This could facilitate determination of binding parameters for low-affinity ligands. (4) The assay can be conducted at low cell densities, reducing the need to consider ligand depletion for high-affinity interactions. (5) Changes in the fluorescent properties of the ligand-associated fluorophore upon binding allow probing of the physical properties of the ligand binding site on the receptor. (6) Different behaviors of subpopulations of cells can be distinguished using the flow cytometer. (7) The assay is readily adaptable to kinetic measurements, including rapid kinetics (*20*, *22*). (8) The assay can be adapted to high-throughput screening for mutant receptors with altered ligand-binding properties similar to screens used by Wittrup and co-workers for yeast-expressed antibodies (*23*).

Equilibrium binding studies using this assay found an increased ligand binding affinity of the α-factor receptor in cells that express high levels of receptors but fail to express G protein subunits, compared with isogenic strains expressing normal levels of G protein. The increase in affinity was greatest for cells expressing high levels of C-terminal-truncated receptors (Table 4). While this result appears superficially to contradict the common paradigm for GPCRs, in which association with G protein enhances ligand affinity, and is at variance with a previous report that receptor affinity for ligand decreases in the absence of G protein subunits (*45*), the discrepancy probably stems from the fact that the previous report assayed binding to isolated membranes, whereas the current work deals with whole-cell assays. In membrane fractions that are depleted of guanine nucleotides, receptors and G proteins can be maintained in a state with high affinity for ligand. In whole cells, where the receptor is likely to maintain interactions with other cellular proteins

and small molecules, such a state could be difficult to detect. A previously reported whole cell binding assay using single-copy chromosomal *STE2* alleles found that deletion of G protein subunits led to a small increase in affinity of truncated receptors and a small decrease in affinity of full-length receptors for radiolabeled α-factor (*42*).

Cells expressing truncated receptors and receptors expressed from multicopy plasmids should contain receptors in stoichiometric excess over G proteins (see ref *48*). Thus, there are probably not enough G proteins in the relevant strains to form stable 1:1 complexes that would be lost in the deletion strains, unless the receptor−G protein complexes are large and nonstoichiometric. The increase in affinity caused by loss of G protein might indicate the presence of transient interactions between receptors and G proteins that modulate receptor affinity or an indirect pathway providing positive feedback to receptors as compensation for the loss of the G protein subunits. It is unlikely that the effects of deleting the G protein subunits are caused by disruption of the "preactivation" receptor−G protein complexes that may be responsible for dominant negative effects of certain receptor alleles (*24*, *42*), since formation of these complexes appears to require the C-terminal tail of the α-factor receptor (*42*), which is absent in the strain exhibiting the largest change in affinity upon deletion of the G_α subunit.

Kinetic analysis of [K^7(NBD),Nle^{12}] α-factor binding to receptors strongly supports the idea that the interaction of this agonist with receptors is a multistep process, since the individual binding trajectories are much better fit by a two-step kinetic scheme than by a single binding event, since the aggregate data sets of rates of binding at different concentrations can be fit by a two-step model, and since the changes in the emission spectrum during binding exhibit a component that is opposite in sign to the overall binding-associated blue shift. These findings apply to both full-length and truncated receptors. Based on the shifts in emission spectrum, [K^7(NBD),Nle^{12}] α-factor first localizes to a nonpolar environment, followed by a rearrangement that exposes it to a region of increased polarity. This conclusion is also supported by the results of fitting of the kinetics of ligand binding to truncated receptors that indicates that the strength of fluorescence emission decreases in the LR* state, compared with the LR state (see Experimental Procedures). The second kinetic phase that we detect could be a conformational change in the receptor that leads to activation of G protein. This phase is unlikely to correspond to internalization of receptors, since it is seen during incubations on ice with truncated receptors, conditions under which receptors internalize slowly and very inefficiently. It is also unlikely to correspond to desensitization, since it is seen with truncated receptors that are defective for known modes of desensitization (*39*, *40*).

Multiple-step kinetics has previously been invoked to explain the interactions of other GPCRs with ligands. For example, binding of thyroid releasing hormone (TRH) to its receptor involves interactions of ligand with groups on the receptor that are too far apart to interact with a single bound ligand molecule. This lends support to the proposal that TRH follows a multistep path to reach its ultimate binding site, interacting first with a surface-exposed site, then with a site more deeply buried in the membrane (*49*). In other cases, such as the β_2-adrenergic receptor, multiple kinetic phases are thought to reflect changes in receptor conformation or ligand interactions that lead to activation or desensitization of signal transduction after the initial binding event (*4*, *6*). In the case of the tachykinin NK2 receptor, binding of fluorescent neurokinin A to the receptor can lead to multiple distinct conformational states with different signaling and functional properties (*50*).

In the case of the α-factor receptor, the polarity of the environment of the ligand appears to first decrease then increase. This could reflect an initial insertion of ligand into a lipid environment, followed by transfer to a binding site on protein (*51*). However, the lack of nonspecific binding to lipids in *ste2*-Δ cells and the high affinity of the binding constants for the initial binding event obtained from global fitting of the kinetic data ($\sim 10^{-7}-10^{-8}$ M^{-1}) indicate that insertion into the lipid environment, if it occurs, involves specific interactions with receptors and not simple partitioning into membranes. The changes in polarity argue against a binding pathway involving initial binding at the membrane surface followed by binding at a deeper site (like that proposed for TRH) unless the local environments of the particular sites in the proteinaceous receptor do not correlate directly with their depth in the membrane. The relationships between the multiple phases of ligand binding and activation or inhibition of receptor signaling is the subject of ongoing studies in this system using various ligand analogues and mutated receptors.

ACKNOWLEDGMENT

We thank Sara Connelly for technical assistance and suggestions and Negin P. Martin for providing the *STE4* knockout construct. Flow cytometry was performed using facilities of the Cancer Center of the University of Rochester, supported by technical assistance and excellent advice from Dr. Peter Keng and the staff of the Center. Fluorescence microscopy was performed using the facilities of Dr. Patricia Hinkle and benefited from her excellent suggestions.

REFERENCES

1. Gether, U., and Kobilka, B. K. (1998) G protein-coupled receptors. II. Mechanism of agonist activation, *J. Biol. Chem. 273*, 17979−82.
2. Lecat, S., Bucher, B., Mely, Y., and Galzi, J. L. (2002) Mutations in the extracellular amino-terminal domain of the NK2 neurokinin receptor abolish cAMP signaling but preserve intracellular calcium responses, *J. Biol. Chem. 277*, 42034−48.
3. Tairi, A. P., Hovius, R., Pick, H., Blasey, H., Bernard, A., Surprenant, A., Lundstrom, K., and Vogel, H. (1998) Ligand binding to the serotonin 5HT3 receptor studied with a novel fluorescent ligand, *Biochemistry 37*, 15850−64.
4. Swaminath, G., Xiang, Y., Lee, T. W., Steenhuis, J., Parnot, C., and Kobilka, B. K. (2004) Sequential binding of agonists to the beta2 adrenoceptor. Kinetic evidence for intermediate conformational states, *J. Biol. Chem. 279*, 686−91.
5. Colson, A. O., Perlman, J. H., Smolyar, A., Gershengorn, M. C., and Osman, R. (1998) Static and dynamic roles of extracellular loops in G-protein-coupled receptors: a mechanism for sequential binding of thyrotropin-releasing hormone to its receptor, *Biophys. J. 74*, 1087−100.
6. Ghanouni, P., Gryczynski, Z., Steenhuis, J. J., Lee, T. W., Farrens, D. L., Lakowicz, J. R., and Kobilka, B. K. (2001) Functionally different agonists induce distinct conformations in the G protein coupling domain of the beta 2 adrenergic receptor, *J. Biol. Chem. 276*, 24433−6.

7. Anderegg, R. J., Betz, R., Carr, S. A., Crabb, J. W., and Duntze, W. (1988) Structure of *Saccharomyces cerevisiae* mating hormone a-factor. Identification of S-farnesyl cysteine as a structural component, *J. Biol. Chem. 263*, 18236−40.
8. Xue, C. B., Caldwell, G. A., Becker, J. M., and Naider, F. (1989) Total synthesis of the lipopeptide a-mating factor of *Saccharomyces cerevisiae*, *Biochem. Biophys. Res. Commun. 162*, 253−7.
9. Zhang, Y. L., Lu, H. F., Becker, J. M., and Naider, F. (1997) Position one analogues of the *Saccharomyces cerevisiae* tridecapeptide pheromone, *J. Pept. Res. 50*, 319−28.
10. Abel, M. G., Zhang, Y. L., Lu, H. F., Naider, F., and Becker, J. M. (1998) Structure−function analysis of the *Saccharomyces cerevisiae* tridecapeptide pheromone using alanine-scanned analogues, *J. Pept. Res. 52*, 95−106.
11. Naider, F., and Becker, J. M. (1986) Structure−activity relationships of the yeast alpha-factor, *CRC Crit. Rev. Biochem. 21*, 225−48.
12. Raths, S. K., Naider, F., and Becker, J. M. (1988) Peptide analogues compete with the binding of alpha-factor to its receptor in *Saccharomyces cerevisiae*, *J. Biol. Chem. 263*, 17333−41.
13. Jenness, D. D., Burkholder, A. C., and Hartwell, L. H. (1983) Binding of alpha-factor pheromone to yeast a cells: chemical and genetic evidence for an alpha-factor receptor, *Cell 35*, 521−9.
14. Jenness, D. D., Burkholder, A. C., and Hartwell, L. H. (1986) Binding of alpha-factor pheromone to *Saccharomyces cerevisiae* a cells: dissociation constant and number of binding sites, *Mol. Cell. Biol. 6*, 318−20.
15. Liu, S., Henry, L. K., Lee, B. K., Wang, S. H., Arshava, B., Becker, J. M., and Naider, F. (2000) Position 13 analogues of the tridecapeptide mating pheromone from *Saccharomyces cerevisiae*: design of an iodinatable ligand for receptor binding, *J. Pept. Res. 56*, 24−34.
16. Siegel, E. G., Gunther, R., Schafer, H., Folsch, U. R., and Schmidt, W. E. (1999) Characterization of novel peptide agonists of the alpha mating factor of *Saccharomyces cerevisiae*, *Anal. Biochem. 275*, 109−15.
17. Sherrill, C., Khouri, O., Zeman, S., and Roise, D. (1995) Synthesis and biological activity of fluorescent yeast pheromones, *Biochemistry 34*, 3553−60.
18. Ding, F. X., Lee, B. K., Hauser, M., Davenport, L., Becker, J. M., and Naider, F. (2001) Probing the binding domain of the *Saccharomyces cerevisiae* alpha-mating factor receptor with fluorescent ligands, *Biochemistry 40*, 1102−8.
19. Ding, F. X., Patri, R., Arshava, B., Naider, F., Lee, B. K., Hauser, M., and Becker, J. M. (2002) Study of the binding environment of alpha-factor in its G protein- coupled receptor using fluorescence spectroscopy, *J. Pept. Res. 60*, 65−74.
20. Sklar, L. A., Edwards, B. S., Graves, S. W., Nolan, J. P., and Prossnitz, E. R. (2002) Flow cytometric analysis of ligand−receptor interactions and molecular assemblies, *Annu. Rev. Biophys. Biomol. Struct. 31*, 97−119.
21. Sklar, L. A., Finney, D. A., Oades, Z. G., Jesaitis, A. J., Painter, R. G., and Cochrane, C. G. (1984) The dynamics of ligand−receptor interactions. Real-time analyses of association, dissociation, and internalization of an N-formyl peptide and its receptors on the human neutrophil, *J. Biol. Chem. 259*, 5661−9.
22. Nolan, J. P., and Sklar, L. A. (1998) The emergence of flow cytometry for sensitive, real-time measurements of molecular interactions, *Nat. Biotechnol. 16*, 633−8.
23. VanAntwerp, J. J., and Wittrup, K. D. (2000) Fine affinity discrimination by yeast surface display and flow cytometry, *Biotechnol. Prog. 16*, 31−7.
24. Leavitt, L. M., Macaluso, C. R., Kim, K. S., Martin, N. P., and Dumont, M. E. (1999) Dominant negative mutations in the alpha-factor receptor, a G protein-coupled receptor encoded by the STE2 gene of the yeast *Saccharomyces cerevisiae*, *Mol. Gen. Genet. 261*, 917−32.
25. Sommers, C. M., Martin, N. P., Akal-Strader, A., Becker, J. M., Naider, F., and Dumont, M. E. (2000) A limited spectrum of mutations causes constitutive activation of the yeast alpha-factor receptor, *Biochemistry 39*, 6898−909.
26. Bonneaud, N., Ozier-Kalogeropoulos, O., Li, G. Y., Labouesse, M., Minvielle-Sebastia, L., and Lacroute, F. (1991) A family of low and high copy replicative, integrative and single-stranded *S. cerevisiae*/*E. coli* shuttle vectors, *Yeast 7*, 609−15.
27. Martin, N. P., Celic, A., and Dumont, M. E. (2002) Mutagenic mapping of helical structures in the transmembrane segments of the yeast alpha-factor receptor, *J. Mol. Biol. 317*, 765−88.
28. Martin, N. P., Leavitt, L. M., Sommers, C. M., and Dumont, M. E. (1999) Assembly of G protein-coupled receptors from fragments: identification of functional receptors with discontinuities in each of the loops connecting transmembrane segments, *Biochemistry 38*, 682−95.
29. Lin, J. C., Parrish, W., Eilers, M., Smith, S. O., and Konopka, J. B. (2003) Aromatic residues at the extracellular ends of transmembrane domains 5 and 6 promote ligand activation of the G protein-coupled alpha-factor receptor, *Biochemistry 42*, 293−301.
30. Akal-Strader, A., Khare, S., Xu, D., Naider, F., and Becker, J. M. (2002) Residues in the first extracellular loop of a G protein-coupled receptor play a role in signal transduction, *J. Biol. Chem. 277*, 30581−90.
31. Alani, E., Cao, L., and Kleckner, N. (1987) A method for gene disruption that allows repeated use of URA3 selection in the construction of multiply disrupted yeast strains, *Genetics 116*, 541−5.
32. Chen, D. C., Yang, B. C., and Kuo, T. T. (1992) One-step transformation of yeast in stationary phase, *Curr. Genet. 21*, 83−4.
33. Rose, M. D., Winston, F. and Hieter, P. (1990) *Methods in Yeast Genetics*, Cold Spring Harbor Laboratory, Cold Spring Harbor, NY.
34. Gietz, R. D., and Sugino, A. (1988) New yeast-*Escherichia coli* shuttle vectors constructed with in vitro mutagenized yeast genes lacking six-base pair restriction sites, *Gene 74*, 527−34.
35. Celic, A., Martin, N. P., Son, C. D., Becker, J. M., Naider, F., and Dumont, M. E. (2003) Sequences in the intracellular loops of the yeast pheromone receptor Ste2p required for G protein activation, *Biochemistry 42*, 3004−17.
36. Kuzmic, P. (1996) Program DYNAFIT for the analysis of enzyme kinetic data: application to HIV proteinase, *Anal. Biochem 237*, 260−73.
37. Yesilaltay, A., and Jenness, D. D. (2000) Homo-oligomeric complexes of the yeast alpha-factor pheromone receptor are functional units of endocytosis, *Mol. Biol. Cell 11*, 2873−84.
38. Stefan, C. J., Overton, M. C., and Blumer, K. J. (1998) Mechanisms governing the activation and trafficking of yeast G protein-coupled receptors, *Mol. Biol. Cell 9*, 885−99.
39. Reneke, J. E., Blumer, K. J., Courchesne, W. E., and Thorner, J. (1988) The carboxy-terminal segment of the yeast alpha-factor receptor is a regulatory domain, *Cell 55*, 221−34.
40. Konopka, J. B., Jenness, D. D., and Hartwell, L. H. (1988) The C-terminus of the *S. cerevisiae* alpha-pheromone receptor mediates an adaptive response to pheromone, *Cell 54*, 609−20.
41. Riezman, H. (1985) Endocytosis in yeast: several of the yeast secretory mutants are defective in endocytosis, *Cell 40*, 1001−9.
42. Dosil, M., Schandel, K. A., Gupta, E., Jenness, D. D., and Konopka, J. B. (2000) The C terminus of the *Saccharomyces cerevisiae* alpha-factor receptor contributes to the formation of preactivation complexes with its cognate G protein, *Mol. Cell. Biol. 20*, 5321−9.
43. Biggar, S. R., and Crabtree, G. R. (2001) Cell signaling can direct either binary or graded transcriptional responses, *EMBO J. 20*, 3167−76.
44. Samama, P., Cotecchia, S., Costa, T., and Lefkowitz, R. J. (1993) A mutation-induced activated state of the beta 2-adrenergic receptor. Extending the ternary complex model, *J. Biol. Chem. 268*, 4625−36.
45. Blumer, K. J., and Thorner, J. (1990) Beta and gamma subunits of a yeast guanine nucleotide-binding protein are not essential for membrane association of the alpha subunit but are required for receptor coupling, *Proc. Natl. Acad. Sci. U.S.A. 87*, 4363−7.
46. Sklar, L. A., and Finney, D. A. (1982) Analysis of ligand−receptor interactions with the fluorescence activated cell sorter, *Cytometry 3*, 161−5.
47. Schandel, K. A., and Jenness, D. D. (1994) Direct evidence for ligand-induced internalization of the yeast alpha-factor pheromone receptor, *Mol. Cell. Biol. 14*, 7245−55.
48. Hao, N., Yildirim, N., Wang, Y., Elston, T. C., and Dohlman, H. G. (2003) Regulators of G protein signaling and transient activation of signaling: experimental and computational analysis reveals negative and positive feedback controls on G protein activity, *J. Biol. Chem. 278*, 46506−15.
49. Perlman, J. H., Colson, A. O., Jain, R., Czyzewski, B., Cohen, L. A., Osman, R., and Gershengorn, M. C. (1997) Role of the extracellular loops of the thyrotropin-releasing hormone receptor: evidence for an initial interaction with thyrotropin-releasing hormone, *Biochemistry 36*, 15670−6.

50. Palanche, T., Ilien, B., Zoffmann, S., Reck, M. P., Bucher, B., Edelstein, S. J., and Galzi, J. L. (2001) The neurokinin A receptor activates calcium and cAMP responses through distinct conformational states, *J. Biol. Chem. 276*, 34853−61.

51. Sargent, D. F., and Schwyzer, R. (1986) Membrane lipid phase as catalyst for peptide-receptor interactions, *Proc. Natl. Acad. Sci. U.S.A. 83*, 5774−8.

BI0494018